Article

Synthesis and Reactivity of a (μ-1,1-Hydroperoxo)(μ-hydroxo)dicopper(II) Complex: Ligand Hydroxylation by a Bridging Hydroperoxo Ligand

Kyosuke Itoh, Hideki Hayashi, Hideki Furutachi, Takahiro Matsumoto, Shigenori Nagatomo, Takehiko Tosha, Shoichi Terada, Shuhei Fujinami, Masatatsu Suzuki, and Teizo Kitagawa

J. Am. Chem. Soc., **2005**, 127 (14), 5212-5223• DOI: 10.1021/ja047437h • Publication Date (Web): 11 March 2005

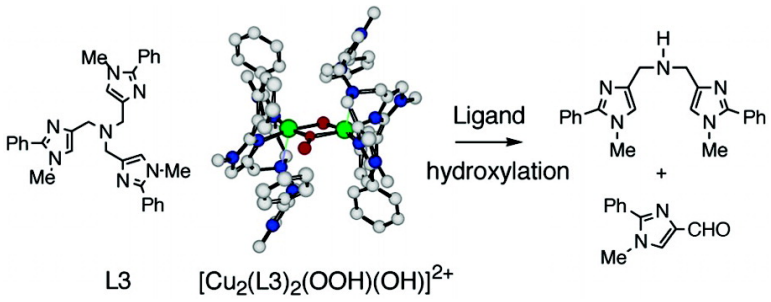

More About This Article

Additional resources and features associated with this article are available within the HTML version:

- Supporting Information
- Links to the 6 articles that cite this article, as of the time of this article download
- Access to high resolution figures
- Links to articles and content related to this article
- Copyright permission to reproduce figures and/or text from this article

View the Full Text HTML

J|A|C|S
ARTICLES
Published on Web 03/11/2005

Synthesis and Reactivity of a (μ-1,1-Hydroperoxo)(μ-hydroxo)dicopper(II) Complex: Ligand Hydroxylation by a Bridging Hydroperoxo Ligand

Kyosuke Itoh,[†] Hideki Hayashi,[†] Hideki Furutachi,[†] Takahiro Matsumoto,[†] Shigenori Nagatomo,[‡] Takehiko Tosha,[‡] Shoichi Terada,[†] Shuhei Fujinami,[†] Masatatsu Suzuki,*[,†] and Teizo Kitagawa[‡]

Contribution from the Department of Chemistry, Faculty of Science, Kanazawa University, Kakuma-machi, Kanazawa 920-1192, Japan, and Center for Integrative Bioscience, Okazaki National Research Institutes, Myodaiji, Okazaki, 444-8585 Japan

Received May 1, 2004; Revised Manuscript Received January 25, 2005; E-mail: suzuki@cacheibm.s.kanazawa-u.ac.jp

Abstract: A new tetradentate tripodal ligand (L3) containing sterically bulky imidazolyl groups was synthesized, where L3 is tris(1-methyl-2-phenyl-4-imidazolylmethyl)amine. Reaction of a bis(μ-hydroxo)-dicopper(II) complex, $[Cu_2(L3)_2(OH)_2]^{2+}$ (**1**), with H_2O_2 in acetonitrile at −40 °C generated a (μ-1,1-hydroperoxo)dicopper(II) complex $[Cu_2(L3)_2(OOH)(OH)]^{2+}$ (**2**), which was characterized by various physicochemical measurements including X-ray crystallography. The crystal structure of **2** revealed that the complex cation has a Cu_2(μ-1,1-OOH)(μ-OH) core and each copper has a square pyramidal structure having an N_3O_2 donor set with a weak ligation of a tertiary amine nitrogen in the apex. Consequently, one pendant arm of L3 in **2** is free from coordination, which produces a hydrophobic cavity around the Cu_2(μ-1,1-OOH)(μ-OH) core. The hydrophobic cavity is preserved by hydrogen bondings between the hydroperoxide and the imidazole nitrogen of an uncoordinated pendant arm in one side and the hydroxide and the imidazole nitrogen of an uncoordinated pendant arm in the other side. The hydrophobic cavity significantly suppresses the H/D and $^{16}O/^{18}O$ exchange reactions in **2** compared to that in **1** and stabilizes the Cu_2(μ-1,1-OOH)(μ-OH) core against decomposition. Decomposition of **2** in acetonitrile at 0 °C proceeded mainly via disproportionation of the hydroperoxo ligand and reduction of **2** to $[Cu(L3)]^+$ by hydroperoxo ligand. In contrast, decomposition of a solid sample of **2** at 60 °C gave a complex having a hydroxylated ligand $[Cu_2(L3)(L3\text{-}OH)(OH)_2]^{2+}$ (**2**-(L3-OH)) as a main product, where L3-OH is an oxidized ligand in which one of the methylene groups of the pendant arms is hydroxylated. ESI-TOF/MS measurement showed that complex **2**-(L3-OH) is stable in acetonitrile at −40 °C, whereas warming **2**-(L3-OH) at room temperature resulted in the N-dealkylation from L3-OH to give an N-dealkylated ligand, bis(1-methyl-2-phenyl-4-imidazolylmethyl)amine (L2) in ∼80% yield based on **2**, and 1-methyl-2-phenyl-4-formylimidazole (Phim-CHO). Isotope labeling experiments confirmed that the oxygen atom in both L3-OH and Phim-CHO come from OOH. This aliphatic hydroxylation performed by **2** is in marked contrast to the arene hydroxylation reported for some (μ-1,1-hydroperoxo)dicopper(II) complexes with a xylyl linker.

Introduction

Chemistry of mono- and dicopper complexes having active oxygen species is of current interest for understanding the reaction mechanisms of dioxygen activating copper proteins in biological systems and utilizing metal complexes as oxidation catalysts. Hydroperoxo−copper(II) species have been proposed as one of the key intermediates for aliphatic hydroxylation reactions performed by dopamine β-monooxygenase (DβM) and peptidylglycine α-hydroxylating enzyme (PHM).[1−7] Very recently, the crystal structure of a superoxo−$Cu(II)_B$ species has been reported for PHM.[6] This superoxo−Cu(II) or peroxo−copper(II) species generated by the electron transfer from Cu_A has been proposed as an active species for H-atom abstraction from substrate, and the resulting hydroperoxo−copper(II) species plays a role for OH transfer to substrate radical.[6,7] A dinuclear (μ-1,1-OOH)Cu(I)Cu(II) species has also been suggested as one possible reaction intermediate for multicopper oxidases such as laccase.[8] Many mononuclear Cu(II)−OOR (R = H, alkyl, or acyl) complexes have been developed, and they have provided fundamental insights into the spectroscopic and

[†] Kanazawa University.
[‡] Okazaki National Research Institutes.

(1) Klinman, J. P. *Chem. Rev.* **1996**, *96*, 2541−2561.
(2) Evans, J. P.; Ahn, K.; Klinman, J. P. *J. Biol. Chem.* **2003**, *278*, 49691−49698.
(3) Prigge, S. T.; Kolhekar, A. S.; Eipper, B. A.; Mains, R. E.; Amzel, L. M. *Science* **1997**, *278*, 1300−1305.
(4) Francisco, W. A.; Blackburn, N. J.; Klinman, J. P. *Biochemistry* **2003**, *42*, 1813−1819.
(5) Bell, J.; Meskini, R. E.; D′Amato, D.; Mains, R. E.; Eipper, B. A. *Biochemistry* **2003**, *42*, 7133−7142.
(6) Prigge, S. T.; Eipper, B. A.; Mains, R. E.; Amzel, L. M. *Science* **2004**, *304*, 864−867.
(7) Chen, P.; Solomon, E. I. *J. Am. Chem. Soc.* **2004**, *126*, 4991−5000.
(8) Solomon, E. I.; Chen, P.; Metz, M.; Lee, S.-K.; Palmer, A. E. *Angew. Chem., Int. Ed.* **2001**, *40*, 4570−4590.

10.1021/ja047437h CCC: $30.25

structural properties.[9−21] In addition, oxidation reactions of various substrates such as $(R)_2S$, $(R)_2SO$, PPh_3, cyclohexene, and cyclohexane have also been reported for some complexes.[11,13,17−21] It has been shown that sterically demanding dinucleating ligands generate dinuclear μ-1,1-hydroperoxo or acylperoxo−dicopper(II) complexes.[22−29] (μ-1,1-Hydroperoxo)dicopper(II) species (Cu_2−OOH) have been shown to be reactive for oxo transfer toward nucleophilic substrates such as PPh_3 and $(R)_2S$.[9,22,27] Furthermore, Cu_2−OOH species have been proposed as reactive intermediates for arene hydroxylation of *m*-xylyl linkers of some dicopper complexes.[23,28] Karlin and co-workers suggested the formation of a Cu_2−OOH species generated by the reaction of a dinuclear copper(II) complex $[Cu_2LH]^{4+}$ [30] with H_2O_2. The Cu_2−OOH species is further activated by an intermolecular mechanism that involves the participation of an additional $[Cu_2LH]^{4+}$, leading to the hydroxylation of a xylyl linker.[23] For a closely related dinucleating ligand having benzimidazolyl groups instead of pyridyl groups, Casella and co-workers have also reported the arene hydroxylation. However, unlike the $[Cu_2LH]^{4+}$ system, double hydroxylation of a xylyl linker occurs in their complex ($[Cu_2L]^{4+}$). For this hydroxylation reaction, a Cu_2−OOH species has also been proposed as a reactive intermediate. The hydroxylation has been suggested to proceed through a direct overlap between the arene HOMO and the peroxide σ^* component.[28] However, the Cu_2−OOH intermediates proposed in the above hydroxylation reactions are not fully characterized. To obtain further insight into the reactivity of the Cu_2−OOH species, it is necessary to synthesize a reasonably stable complex, which can be characterized by various physicochemical measurements and is capable of arene or aliphatic hydroxylation, although no aliphatic hydroxylation by $Cu(II)_2$−OOR species has been reported thus far.

Scheme 1. Synthetic Procedures of Ligands and (μ-1,1-Hydroperoxo)(μ-hydroxo)dicopper(II) Complexes and Abbreviations of Complexes

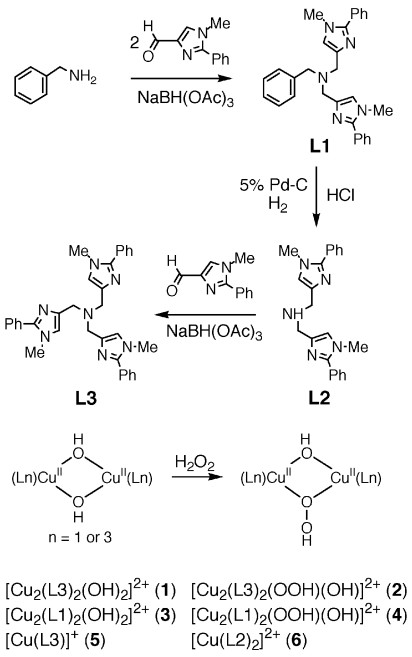

$[Cu_2(L3)_2(OH)_2]^{2+}$ (**1**) $[Cu_2(L3)_2(OOH)(OH)]^{2+}$ (**2**)
$[Cu_2(L1)_2(OH)_2]^{2+}$ (**3**) $[Cu_2(L1)_2(OOH)(OH)]^{2+}$ (**4**)
$[Cu(L3)]^{+}$ (**5**) $[Cu(L2)_2]^{2+}$ (**6**)

In this study, we synthesized a new sterically hindered tetradentate tripodal ligand (L3) having a 2-phenylimidazolyl group as shown in Scheme 1, in which phenyl group is introduced as a reaction probe and/or a constituent forming a hydrophobic cavity. The ligand L3 forms a dinuclear bis(μ-hydroxo)dicopper(II) complex, $[Cu_2(L3)_2(OH)_2]^{2+}$ (**1**), which reacts with H_2O_2 in acetonitrile at −40 °C to produce a (μ-1,1-hydroperoxo)(μ-hydroxo)dicopper(II) complex $[Cu_2(L3)_2(OOH)(OH)]^{2+}$ (**2**). Complex **2** was spectroscopically and structurally characterized, and its reactivity was investigated. Decomposition of **2** in solid state resulted in hydroxylation of the methylene group of L3. This is the first example of aliphatic hydroxylation of the supporting ligand by Cu_2−OOH species.

Experimental Section

Materials. All reagents and solvents were obtained from commercial sources and used without further purification except for ligand-recovering experiments and spectroscopic measurements. $H_2{}^{18}O_2$ was prepared by the literature methods.[31] Acetonitrile and acetone were dried over molecular sieves 5A and distilled under N_2 atmosphere before use.

Syntheses of Ligands. 1-Methyl-2-phenyl-4-formylimidazole (PhimCHO). To a suspension of NaH (60% oil dispersion, 5.80 g, 145 mmol) in 200 mL of dry DMF at 0 °C was added dropwise 2-phenyl-4-

(9) Karlin, K. D.; Zuberbühler, A. D. In *Bioinorganic Catalysis*, 2nd ed.; Reedijk, J., Bouwman, E., Eds.; Marcel Dekker: New York, 1999; pp 469−534.
(10) Wada, A.; Harata, M.; Hasegawa, K.; Jitsukawa, K.; Masuda, H.; Mukai, M.; Kitagawa, T.; Einaga, H. *Angew. Chem., Int. Ed.* **1998**, *37*, 798−799.
(11) Chen, P.; Fujisawa, K.; Solomon, E. I. *J. Am. Chem. Soc.* **2000**, *122*, 10177−10193.
(12) Ohtsu, H.; Itoh, S.; Nagatomo, S.; Kitagawa, T.; Ogo, S.; Watanabe, Y.; Fukuzumi, S. *Chem. Commun*. **2000**, 1051−1052.
(13) Ohta, T.; Tachiyama, T.; Yoshizawa, K.; Yamabe, T.; Uchida, T.; Kitagawa, T. *Inorg. Chem*. **2000**, *39*, 4358−4369.
(14) Ohtsu, H.; Itoh, S.; Nagatomo, S.; Kitagawa, T.; Ogo, S.; Watanabe, Y.; Fukuzumi, S. *Inorg. Chem.* **2001**, *40*, 3200−3207.
(15) Kodera, M.; Kita, T.; Miura, I.; Nakayama, N.; Kawata, T.; Kano, K.; Hirota, S. *J. Am. Chem. Soc*. **2001**, *123*, 7715−7716.
(16) Osako, T.; Nagatomo, S.; Tachi, Y.; Kitagawa, T.; Itoh, S. *Angew. Chem., Int. Ed*. **2002**, *41*, 4325−4328.
(17) Fujii, T.; Naito, A.; Yamaguchi, S.; Wada, A.; Funahashi, Y.; Jitsukawa, K. Nagatomo, S.; Kitagawa, T.; Masuda, H. *Chem. Commun*. **2003**, 2700−2701.
(18) Yamaguchi, S.; Nagatomo, S.; Kitagawa, T.; Funahashi, Y.; Ozawa, T.; Jitsukawa, K.; Masuda, H. *Inorg. Chem*. **2003**, *42*, 6968−6970.
(19) Kitajima, N.; Katayama, T.; Fujisawa, K.; Iwata, Y.; Morooka, Y. *J. Am. Chem. Soc.* **1993**, *115*, 7872−7873.
(20) Kitajima, N.; Fujisawa, K.; Moro-oka, Y. *Inorg. Chem.* **1990**, *29*, 357−358.
(21) Sanyal, I.; Ghosh, P.; Karlin, K. D. *Inorg. Chem*. **1995**, *34*, 3050−3056.
(22) Karlin, K. D.; Ghosh, P.; Cruse, R. W.; Farooq, A.; Gultneh, Y.; Jacobson, R. R.; Blackburn, N. J.; Strange, R. W.; Zubieta, J. *J. Am. Chem. Soc*. **1988**, *110*, 6769−6780.
(23) Cruse, R. W.; Kaderli, S.; Meyer, C. J.; Zuberbühler, A. D.; Karlin, K. D. *J. Am. Chem. Soc*. **1988**, *110*, 5020−5024.
(24) Sorrell, T. N.; Vankai, V. A. *Inorg. Chem.* **1990**, *29*, 1687−1692.
(25) Mahroof-Tahir, M.; Murthy, N. N.; Karlin, K. D.; Blackburn, N. J.; Shaikh, S. N.; Zubieta, J. *Inorg. Chem.* **1992**, *31*, 3001−3003.
(26) Root, D. E.; Mahroof-Tahir, M.; Karlin, K. D.; Solomon, E. I. *Inorg. Chem.* **1998**, *37*, 4838−4848.
(27) Murthy, N. N.; Mahroof-Tahir, M.; Karlin, K. D. *Inorg. Chem.* **2001**, *40*, 628−635.
(28) Battaini, G.; Monzani, E.; Perotti, A.; Para, C.; Casella, L.; Santagostini, L.; Gullotti, M.; Dillinger, R.; Näther, C.; Tuczek, F. *J. Am. Chem. Soc*. **2003**, *125*, 4185−4198.
(29) Ghosh, P.; Tyeklar, Z.; Karlin, K. D.; Jacobson, R. R.; Zubieta, J. *J. Am. Chem. Soc.* **1987**, *109*, 6889−6891.
(30) Abbreviations of ligands, used: LH = α,α′-bis{bis[2-(2-pyridyl)ethyl]-amino}-*m*-xylene; L = α,α′-bis{bis[2-(1′-methyl-2′-benzimidazolyl)ethyl]-amino}-*m*-xylene; tpa = tris(2-pyridylmethyl)amine; bppa = bis(6-pival-amide-2-pyridylmethyl)(2-pyridylmethyl)amine; La = *N*-{2-[(2-bis(2-pyridylmethyl)aminoethyl)methylamino]ethyl}-2,2-dimethylpropion-amide; bpba = bis(2-pyridylmethyl)*tert*-butylamine; N3S = 2-bis(6-methyl-2-pyridylmethyl)amino-1-(phenylthio)ethane; HB(3-tBu-5-^{i}Prpz)$_3$ hydrotris-(3-*tert*-butyl-5-isopropylpyrazolyl)borate anion; Py_2SSPy_2 = bis{2-[*N*,*N*-bis(2-pyridylethyl)-amino]-1,1-dimethylethyl}disulfide); TPPA = tris[(6-phenyl-2-pyridyl)methyl]amine.
(31) Sitter, A. J.; Terner J. *J. Labelled Compd. Radiopharm.* **1985**, *22*, 461−465.

formylimidazole (25.0 g, 145 mmol) with stirring. After evolution of H_2 gas ceased, CH_3I (24.7 g, 174 mmol) was slowly added to the solution with stirring. The resulting solution was stirred for 3 h at 0 °C and then overnight at room temperature to give a yellow suspension. After removal of insoluble material by filtration, DMF was removed under reduced pressure. The residue was suspended in a saturated NaCl aqueous solution (50 mL) and extracted twice with ethyl acetate (100 mL). The combined extracts were dried over Na_2SO_4. The solvent was evaporated under reduced pressure to give a yellow solid, which contained ca. 30% of an undesirable isomer (1-methyl-2-phenyl-5-formylimidazole), which was checked by NMR. The solid was finely powdered and suspended into 200 mL of diethyl ether. The resulting suspension was stirred overnight to dissolve the undesirable isomer. Insoluble Phim-CHO was collected by filtration. Yield: 11.9 g (44%). Anal. Calcd for $C_{11}H_{10}N_2O$: C, 70.95; H, 5.41; N, 15.04%. Found: C, 71.00; H, 5.39; N, 15.03%. ^{1}H NMR ($CDCl_3$, 400 MHz): δ (ppm) = 3.81 (3H, s, 1-CH_3 of imidazole), 7.47−7.52 (3H, m, *m*- and *p*-H of phenyl), 7.64−7.67 (2H, m, *o*-H of phenyl), 7.69 (1H, s, 5-H of imidazole), 9.92 (1H, s, 4-CHO of imidazole). ^{13}C NMR ($CDCl_3$, 100.4 MHz): δ (ppm) = 34.9 (1-CH_3 of imidazole), 128.1 (*p*-C of phenyl), 128.4 (*m*-C of phenyl), 128.6 (*o*-C of phenyl), 129.0 (4-C of imidazole), 129.3 (5-C of imidazole), 140.7 (2-C of imidazole), 149.5 (1-C of phenyl), 185.6 (4-CHO of imidazole). GC/MS: t_R 7.8 min, *m*/*z* (relative intensity): 186 (100), 157 (18), 118 (24). ESI-TOF/MS ($CHCl_3$ solution containing a small amount of formic acid) *m*/*z*: 373.1 (100, $[2M + 1]^+$) 187.1 (35, $[M + 1]^+$).

Bis(1-methyl-2-phenyl-4-imidazolylmethyl)benzylamine·H_2O (L1). To a THF solution (100 mL) containing 1-methyl-2-phenyl-4-formylimidazole (Phim-CHO) (10.24 g, 55.0 mmol) and benzylamine (5.89 g, 55.0 mmol) was added $NaBH(OAc)_3$ (34.97 g, 165 mmol). After the suspension was stirred overnight, acetic acid (3.30 g, 55.0 mmol) and another Phim-CHO (10.24 g, 55.0 mmol) was added to the solution. After being stirred for 6 h, the solution was made basic by addition of an aqueous NaOH solution. THF was removed under reduced pressure. To the residue was added a saturated NaCl aqueous solution (50 mL), and an oily layer separated was extracted twice with chloroform (100 mL). The combined chloroform extracts were dried over Na_2SO_4. After filtration, chloroform was evaporated under reduced pressure to give a brown oil that was dissolved in an ethyl acetate/diethyl ether mixture. The solution was allowed to stand overnight to give a white powder. Yield: 19.2 g (75%). Anal. Calcd for $C_{29}H_{31}N_5O$: C, 74.81; H, 6.71; N, 15.04%. Found: C, 74.81; H, 6.68; N, 15.01%. ^{1}H NMR ($CDCl_3$, 400 MHz): δ (ppm) = 3.63 (6H, s, 1-CH_3 of imidazole), 3.75 (4H, s, 4-CH_2 of imidazole), 3.77 (2H, s, CH_2 of benzyl), 6.96 (2H, s, 5-H of imidazole), 7.20 (1H, t, *p*-H of benzyl), 7.30 (2H, t, *m*-H of benzyl), 7.35−7.40 (6H, m, *m*- and *p*-H of phenyl), 7.45 (2H, d, *o*-H of benzyl), 7.59 (4H, d, *o*-H of phenyl). ^{13}C NMR ($CDCl_3$, 100.4 MHz): δ (ppm) = 34.1 (1-CH_3 of imidazole), 51.0 (4-CH_2 of imidazole), 57.6 (CH_2 of benzyl), 120.6 (5-C of imidazole), 126.4 (*p*-C of benzyl), 127.9 (*m*-C of benzyl), 128.2 (*m*- and *p*-C of phenyl), 128.4 (*o*-C of phenyl), 128.7 (*o*-C of benzyl), 130.4 (4-C of imidazole), 138.8 (1-C of benzyl), 139.7 (2-C of imidazole), 146.7 (1-C of phenyl). GC/MS: t_R 25.3 min, *m*/*z* (relative intensity): 276 (100), 171 (85), 157 (26). ESI-TOF/MS ($CHCl_3$ solution containing a small amount of formic acid) *m*/*z*: 448.2 (100, $[M + 1]^+$).

Bis(1-methyl-2-phenyl-4-imidazolylmethyl)amine·0.5H_2O (L2). Removal of a benzyl group from L1 was achieved by hydrogenation using 5% Pd−C and H_2. To a methanol solution (100 mL) containing L1 (13.97 g, 30.0 mmol) and concentrated HCl (10 mL) was added 5% Pd−C (ca. 2 g). H_2 gas was introduced into the system, and the resulting suspension was vigorously stirred for 7 h at 40 °C. After removal of Pd−C by filtration, the solution was made basic by addition of an aqueous NaOH solution. The solvent was evaporated under reduced pressure. The residue was suspended in a saturated aqueous NaCl solution (50 mL) and extracted by $CHCl_3$ (100 mL) three times. The combined chloroform extracts were dried over Na_2SO_4. After filtration, chloroform was removed under reduced pressure to give a pale brown powder, which was used for the subsequent reaction without purification. Yield: 10.6 g (96%). Anal. Calcd for $C_{22}H_{24}N_5O_{0.5}$: C, 72.11; H, 6.60; N, 19.11%. Found: C, 72.07; H, 6.68; N, 18.89%. ^{1}H NMR ($CDCl_3$, 400 MHz): δ (ppm) = 3.67 (6H, s, 1-CH_3 of imidazole), 3.86 (4H, s, 4-CH_2 of imidazole), 6.90 (2H, s, 5-H of imidazole), 7.37 (2H, t, *p*-H of phenyl), 7.43 (4H, t, *m*-H of phenyl), 7.60 (4H, d, *o*-H of phenyl). ^{13}C NMR ($CDCl_3$, 100.4 MHz): δ (ppm) = 34.3 (1-CH_3 of imidazole), 46.7 (4-CH_2 of imidazole), 119.7 (5-C of imidazole), 128.4 (*m*-C of phenyl), 128.5 (*p*-C of phenyl), 128.7 (*o*-C of phenyl), 130.6 (4-C of imidazole), 140.2 (2-C of imidazole), 147.4 (1-C of phenyl). GC/MS: t_R 22.1 min, *m*/*z* (relative intensity): 186 (85), 172 (100), 157 (28). ESI-TOF/MS ($CHCl_3$ solution containing a small amount of formic acid) *m*/*z*: 358.2 (100, $[M + 1]^+$).

Tris(1-methyl-2-phenyl-4-imidazolylmethyl)amine·1.5H_2O (L3). A THF solution (100 mL) containing L2 (12.8 g, 35.0 mmol), Phim-CHO (6.52 g, 35.0 mmol), and acetic acid (2.1 g, 35.0 mmol) was stirred for 5 h. To the resulting solution was added $NaBH(OAc)_3$ (11.2 g, 52.5 mmol), and the suspension was stirred overnight. Then the solution was made basic by addition of an aqueous NaOH solution, and THF was removed by reduced pressure. The residue was suspended in a saturated aqueous NaCl solution (50 mL) and extracted in ethyl acetate (100 mL) three times. The combined extracts were dried over Na_2SO_4. After filtration, ethyl acetate was removed under reduced pressure to give a white powder. Yield: 14.7 g (76%). Anal. Calcd for $C_{33}H_{36}N_7O_{1.5}$: C, 71.46; H, 6.54; N, 17.68%. Found: C, 71.40; H, 6.48; N, 17.21%. ^{1}H NMR ($CDCl_3$, 400 MHz): δ (ppm) = 3.62 (9H, s, 1-CH_3 of imidazole), 3.81 (6H, s, 4-CH_2 of imidazole), 7.10 (3H, s, 5-H of imidazole), 7.32 (3H, t, *p*-H of phenyl), 7.39 (6H, t, *m*-H of phenyl), 7.61 (6H, d, *o*-H of phenyl). ^{13}C NMR ($CDCl_3$, 100.4 MHz): δ (ppm) = 34.4 (1-CH_3 of imidazole), 51.0 (4-CH_2 of imidazole), 121.5 (5-C of imidazole), 128.4 (*p*-C of phenyl), 128.4 (*m*-C of phenyl), 128.6 (*o*-C of phenyl), 130.7 (4-C of imidazole), 138.8 (2-C of imidazole), 146.9 (1-C of phenyl). ESI-TOF/MS ($CHCl_3$ solution containing a small amount of formic acid) *m*/*z*: 528.3 (100, $[M + 1]^+$).

Syntheses of Complexes. Copper(I) and copper(II) complexes were prepared under N_2 atmosphere using Schlenk techniques. *Caution: Perchlorate salts are potentially explosive and should be handled with care.*

$[Cu_2(L3)_2(OH)_2](CF_3SO_3)_2$·$(CH_3)_2CO$·$H_2O$ (1-CF_3SO_3). To an acetone solution (20 mL) containing L3 (2.27 g, 4.1 mmol) and $Cu(CF_3SO_3)_2$ (1.44 g, 4.0 mmol) was added Et_3N (1.67 mL, 12.0 mmol) with stirring to give a blue powder, which was filtered, washed with acetone and diethyl ether, and dried in vacuo. Yield: 2.6 g (66%). Anal. Calcd for $C_{71}H_{76}N_{14}Cu_2O_{10}F_6S_2$: C, 53.61; H, 4.82; N, 12.33%. Found: C, 53.57; H, 4.79; N, 12.30%. UV−vis (λ_{max}/nm (ϵ/M^{-1} cm^{-1}) in acetonitrile at room temperature): 590 (80), 690 (sh). FTIR (KBr, cm^{-1}): 1585 (C═C, aromatic), 1479 (imidazole), 1407 (imidazole), 1224 (CF_3SO_3), 1155 (CF_3SO_3), 1031 (CF_3SO_3), 638 (CF_3SO_3). ESI-TOF/MS (acetonitrile solution at room temperature) *m*/*z*: 607.2 $[M]^{2+}$. It was difficult to grow single crystals suitable for X-ray crystallography by recrystallization from acetone. However, recrystallization from acetonitrile gave single crystals ($[Cu_2(L3)_2(OH)_2](CF_3SO_3)_2$·$CH_3CN$ (**1**-CF_3SO_3·CH_3CN)) suitable for X-ray crystallography.

$[Cu_2(L3)_2(OOH)(OH)](CF_3SO_3)_2$ (2-CF_3SO_3). To an acetonitrile solution (20 mL) containing **1**-CF_3SO_3 (148 mg, 0.093 mmol) at −40 °C was added 30% H_2O_2 (40 equiv, 372 μL) with stirring to give a green solution. Diethyl ether was added to the resulting solution to give olive-green powder, which was collected by filtration and washed with diethyl ether and dried in vacuo at −40 °C. Although it was attempted to prepare single crystals suitable for X-ray crystallography by recrystallization from various solvents, all the attempts were in vain. However, BPh_4 salt prepared by metathesis gave single crystals (vide infra). UV−vis (λ_{max}/nm (ϵ/M^{-1} cm^{-1}) in acetonitrile at −40 °C): 356 (6300) and 580 (240). ESI-TOF/MS (acetonitrile solution at −40 °C) *m*/*z*: 615.2 $[M]^{2+}$.

$[Cu_2(L3)_2(OOH)(OH)](BPh_4)_2\cdot 5(CH_3)_2CO\cdot 3H_2O$ (2-BPh_4). Complex **2**-CF_3SO_3 (ca. 100 mg) was dissolved in a small amount of acetone at −40 °C, to which was added $NaBPh_4$ (170 mg). The resulting solution was allowed to stand for a few days at −80 °C to give green crystals suitable for X-ray crystallography.

$[Cu_2(L3)_2(^{18}O^{18}OH)(OH)](CF_3SO_3)_2$ (2-($^{18}O^{18}OH$)). This was synthesized by the same method as **2-CF_3SO_3** except $H_2{}^{18}O_2$ was used. ESI-TOF/MS (acetonitrile solution at −40 °C) *m*/*z*: 617.2 $[M]^{2+}$.

$[Cu_2(L1)_2(OH)_2](CF_3SO_3)_2\cdot(CH_3)_2CO\cdot H_2O$ (3-CF_3SO_3). To an acetone solution (10 mL) containing L1 (1.91 g, 4.1 mmol) was added $Cu(CF_3SO_3)_2$ (1.44 g, 4.0 mmol). To this solution was added Et_3N (1.11 mL, 6.0 mmol), and the resulting solution was stirred for 1 h to afford pale blue powder, which was collected by filtration, washed with ethanol and ether, and then dried in vacuo. Yield: 2.4 g (83%). Although it was attempted to obtain single crystals suitable for X-ray crystallography by recrystallization from various solvent, all the attempts were in vain. However, single crystals were obtained as ClO_4 salt (vide infra). Anal. Calcd for $C_{63}H_{68}N_{10}Cu_2O_{10}F_6S_2$: C, 52.90; H, 4.79; N, 9.79%. Found: C, 52.80; H, 4.65; N, 9.63%. UV−vis (λ_{max}/nm (ϵ/M^{-1} cm^{-1}) in CH_3CN at room temperature): 333 (4000), 680 (110). FTIR (KBr, cm^{-1}): 1714 (acetone C═O), 1589 (C═C, aromatic), 1481 (imidazole), 1409 (imidazole), 1224 (CF_3SO_3), 1149 (CF_3SO_3), 1031 (CF_3SO_3), 636 (CF_3SO_3). ESI-TOF/MS (in CH_3CN) *m*/*z*: 527.2 $[M]^{2+}$.

$[Cu_2(L1)_2(OH)_2](ClO_4)_2\cdot 2C_2H_5CN$ (3-$ClO_4\cdot C_2H_5CN$). This was prepared by the same method as **3-CF_3SO_3** except $Cu(ClO_4)_2\cdot 6H_2O$ was used. Single crystals suitable for X-ray analysis were obtained by recrystallization from propionitrile.

$[Cu(L3)]ClO_4\cdot 2H_2O$ (5-ClO_4). A methanol solution (5 mL) of L3 (0.58 g, 1.05 mmol) was added to a methanol solution (5 mL) of $[Cu(CH_3CN)_4]ClO_4$ (0.33 g, 1.0 mmol) to produce a white powder, which was collected by filtration, washed with ethanol and diethyl ether, and then dried in vacuo. Yield: 0.46 g (62%). Anal. Calcd for $C_{33}H_{37}N_7CuO_6Cl$: C, 54.54; H, 5.13; N, 13.49%. Found: C, 54.78; H, 5.15; N, 13.10%. ^{1}H NMR (acetone-d_6, 400 MHz): δ (ppm) = 3.62 (9H, s, 1-CH_3 of imidazol), 3.81 (6H, s, 4-CH_2 of imidazol), 7.10 (3H, s, 5-H of imidazol), 7.32 (3H, t, *p*-H of phenyl), 7.39 (6H, t, *m*-H of phenyl), 7.61 (6H, d, *o*-H of phenyl). FTIR (KBr, cm^{-1}): 1579 (C═C, aromatic), 1477 (imidazole), 1405 (imidazole), 1093 (ClO_4), 626 (ClO_4). ESI-TOF/MS (acetonitrile solution at room temperature) *m*/*z*: 590.2 $[M]^+$.

$[Cu(L2)_2](ClO_4)_2\cdot(CH_3)_2CO$ (6-ClO_4). $Cu(ClO_4)_2\cdot 6H_2O$ (0.19 g, 0.5 mmol) was dissolved into an acetone solution (5 mL) containing L2 (0.19 g, 0.52 mmol). The resulting blue solution was allowed to stand under diethyl ether vapor to give blue crystals, which were collected by filtration, washed with ethanol and diethyl ether, and dried in vacuo. Yield: 0.25 g (48%). Anal. Calcd for $C_{47}H_{52}N_{10}CuO_9Cl_2$: C, 54.52; H, 5.06; N, 13.53%. Found: C, 54.40; H, 5.17; N, 13.49%. UV−vis (λ_{max}/nm (ϵ/M^{-1} cm^{-1}) in CH_3CN at room temperature): 685 (150), ~850 (120). FTIR (KBr, cm^{-1}): 1704 (acetone C═O), 1594 (C═C, aromatic), 1477 (imidazole), 1403 (imidazole), 1095 (ClO_4), 622 (ClO_4). ESI-TOF/MS (in CH_3CN) *m*/*z*: 388.6 $[M]^{2+}$.

Physical Measurements. The electronic spectra were measured with an Otsuka Electronics photodiode array spectrometer MCPD-2000 with an Otsuka Electronics optical fiber attachment or a Shimadzu diode array spectrometer Multispec-1500. The temperatures were controlled with an EYELA low-temperature pair stirrer PSL-1800 for the former instrument and with a Unisoku thermostated cell holder for the latter one. The reflectance spectra were obtained with an Otsuka Electronics photodiode array spectrometer MCPD-2000 with an Otsuka Electronics optical fiber attachment.

Resonance Raman spectra were obtained with a liquid nitrogen cooled CCD detector (model LN/CCD-1340 × 400PB, Princeton Instruments) attached to a 1-m single polychrometor (model MC-100DG, Ritsu Oyo Kogaku). The 406.7-nm line of a Kr^+ laser (model 2060 Spectra Physics) was used as an exciting source. The laser powers used were ~10 mW at the sample points. All measurements were carried out with a spinning cell (1000 rpm) at ~−40 °C. Raman shifts were calibrated with indene, and the accuracy of the peak positions of the Raman bands was ±1 cm^{-1}.

^{1}H NMR spectra were measured with JEOL JNM-LM400. Tetramethylsilane was used as an internal standard. Infrared spectra were obtained by the KBr disk method with a HORIBA FT-200 spectrophotometer. GC/MS analysis was performed on a Shimadzu GCMS-QP5050A GC/MS equipped with a fused silica capillary column (Methyl silicone, 0.32 mm diameter × 25 m, QUADREX corporation). ESI-TOF/MS spectra were measured with a Micromass LCT spectrometer.

Ligand Recovery Experiments after Thermal Decomposition of 2-CF_3SO_3. A solid sample of **2**-CF_3SO_3 (ca. 100 mg) was warmed at 60 °C for 1 h under N_2. The resulting solid was dissolved into 100 mL of acetonitrile in a volumetric flask. A portion (10 mL) was taken up, and the amount of the complex used was determined by spectrophotometric determination of copper (vide infra). Identifications and quantitative analyses of the ligand L3, an N-dealkylated ligand (bis(1-methyl-2-phenyl-4-imidazolylmethyl)amine (L2)), and 1-methyl-2-phenyl-4-formylimidazole (Phim-CHO) were as follows. The remaining solution was evaporated to dryness under reduced pressure. Demetalation was carried out by the reaction with concentrated aqueous NH_4OH (30 mL), and then ligand and its reaction products were extracted into chloroform (3 × 20 mL). The reaction products were identified by ^{1}H NMR and ESI-TOF/MS, and their amounts were determined by ^{1}H NMR by addition of 2,6-dimethyl-*p*-benzoquinone as an internal standard. Total amounts of L3 and L2 recovered were more than 91% for three experiments. Yield of the dealkylated ligand L2 was 79% based on a dimer for three experiments. Phim-CHO was also recovered, which was identified by GC/MS and ESI-TOF/MS. Recovery of Phim-CHO obtained from an ^{18}O-labeled **2**-CF_3SO_3 revealed the presence of ^{18}O. The ESI-TOF/MS spectrum of an acetonitrile solution containing a decomposed sample at room temperature revealed that the oxygen atom of Phim-CHO is ^{18}O (almost quantitative), whereas ^{18}O/^{16}O exchange occurred almost completely after 1 day. It was also found that ~60% of ^{18}O was exchanged by ^{16}O during the ligand recovery experiments mentioned above.

Thermal decomposition in acetonitrile was carried out as follows. Typically **2**-CF_3SO_3 (ca. 100 mg) was dissolved in 50 mL of acetonitrile in a Schlenk tube at 0 °C under N_2, and the solution was allowed to stand for 3 h. After decomposition of the complex, the volume of the resulting solution was adjusted to 100 mL in a volumetric flask by addition of acetonitrile. The following procedures are the same as those described above. Yield of the ligand L3 was more than 92% for three experiments. A trace amount of a dealkylated ligand (L2) was identified by GC/MS and ESI-TOF/MS.

Determination of the Concentration of Copper. A typical procedure is as follows. An acetonitrile solution (10 mL) obtained by the above ligand recovery experiment was diluted by 40 mL of acetonitrile and ca. 40 mL of H_2O, to which was added acetic acid to adjust the pH to ca. 5. To the resulting solution was added ca. 200 mg of ascorbic acid and ca. 300 mg of 2,9-dimethyl-1,10-phenanthroline to generate $[Cu(Me_2\text{-phen})_2]^+$. The volume of the solution was adjusted to 100 mL by addition of H_2O in a volumetric flask. The copper concentration was determined spectrophotometrically by the absorbance at 455 nm (the molar extinction coefficient of $[Cu(Me_2\text{-phen})_2]^+$ under the conditions is 7800 M^{-1} cm^{-1}).

Determination of the Amount of Cu(I) Ion in Decomposed Solution. An acetonitrile solution (20 mL) containing **2**-CF_3SO_3 (ca. 1 mM) was allowed to stand at 0 °C under N_2. After 3 h, a portion (5 mL) was taken up, to which was added ca. 20 mL of acetonitrile/water (1:1) and ca. 50 mg of 2,9-dimethyl-1,10-phenanthroline to generate $[Cu(Me_2\text{-phen})_2]^+$. To the resulting solution was added acetic acid to adjust the pH to ca. 5, and the volume of the solution was adjusted to 50 mL by addition of acetonitrile/water (1:1) in a volumetric flask. The concentration of copper(I) ion was determined spectrophotometri-

Table 1. Crystallographic Data for $[Cu_2(L3)_2(OH)_2](CF_3SO_3)_2\cdot CH_3CN$ (**1**-$CF_3SO_3\cdot CH_3CN$), $[Cu_2(L3)_2(OOH)(OH)](BPh_4)_2\cdot 5(CH_3)_2CO\cdot 3H_2O$ (**2**-BPh_4), and $[Cu_2(L1)_2(OH)_2](ClO_4)_2\cdot 2C_2H_5CN$ (**3**-$ClO_4\cdot C_2H_5CN$)

	1-$CF_3SO_3\cdot CH_3CN$	**2**-BPh_4	**3**-$ClO_4\cdot C_2H_5CN$
formula	$C_{70}H_{71}O_8N_{15}Cu_2S_2F_6$	$C_{129}H_{144}O_{11}N_{14}Cu_2B_2$	$C_{64}H_{70}O_{10}N_{12}Cu_2Cl_2$
temp, °C	−150	−150	−150
mol wt	1555.63	2215.36	1365.33
cryst syst	monoclinic	triclinic	triclinic
space group	*C*2/*c*	$P\bar{1}$	$P\bar{1}$
a, Å	23.989(6)	14.023(5)	11.163(2)
b, Å	16.678(4)	15.810(6)	12.857(2)
c, Å	18.853(5)	17.194(7)	13.130(3)
α, deg		104.038(7)	71.78(3)
β, deg	105.033(6)	101.808(7)	84.60(3)
γ, deg		105.329(8)	64.95(3)
V, Å^3	7284(2)	3416(2)	1619.9(7)
Z	4	1	1
$2\theta_{max}$	55.0	55.0	60.7
F(000)	3216.00	1172.00	710.00
D_{calcd}, g/cm^3	1.418	1.077	1.399
abs. coeff, cm^{-1}	7.21	3.68	8.06
No. of reflns colld	27372	23656	18710
No. of indep reflns	5538 ($I \geq 3.00\sigma(I)$)	8116 ($I \geq 3.00\sigma(I)$)	6698($I \geq 3.00\sigma(I)$)
No. of refined params	463	717	406
GOF indication	1.70	1.89	1.47
largest peak/hole, e Å^{-3}	1.14/−0.64	1.19/−0.62	1.36/−0.69
R^a	0.064	0.088	0.046
$R_w{}^b$	0.095	0.133	0.076

[a] $R = \sum[|F_o| - |F_c|]/\sum|F_o|$ ($I \geq 3.0\sigma(I)$). [b] $R_w = [\sum w(|F_o| - |F_c|)^2/\sum w|F_o|^2]^{1/2}$; $w = 1/[\sigma^2(F_o) + p^2|F_o|^2/4]$ ($p = 0.081$ for **1**-$CF_3SO_3\cdot CH_3CN$, $p = 0.097$ for **2**-BPh_4, and $p = 0.085$ for **3**-$ClO_4\cdot C_2H_5CN$.

cally by the absorbance at 455 nm as described above. Yield of copper(I) ion was ca. 20% for two experiments.

Dioxygen Evolution Analysis upon Decomposition. An apparatus used for the experiment is shown in Figure S1a. Acetonitrile (40 mL) in a vessel (ca. 62 mL) at 0 °C was equilibrated with dry air. After equilibration, the reading of the oxygen sensor was 18.0 ± 0.1%. The amount of dioxygen evolved upon decomposition of **2** was calibrated by injecting the appropriate amounts of O_2 gas (0.2, 0.5, 1.0, 1.3, and 1.5 mL) by a pressure-lock syringe through septum, and the oxygen concentrations were measured after 10 min. A fairly good calibration line was obtained as seen in Figure S1b. A typical experiment was as follows. Complex **2** (ca. 60 mg) was quickly placed on a sample holder from the sample inlet by opening the septum with gentle flowing of dry air. After the system was closed, a solid sample was dropped into acetonitrile by pushing the sample plate by a needle. After 10 min, oxygen concentration was measured. Yield: ca. 40% based on a dimer for two experiments.

X-ray Crystallography. General Procedures. Data collections were carried out on a Rigaku/MSC mercury diffractometer with graphite monochromated Mo Kα radiation ($\lambda = 0.71070$ Å). The data were collected at −150 ± 1 °C to a maximum 2θ value of 55.0° for **1**-$CF_3SO_3\cdot CH_3CN$ and **2**-BPh_4, and to a maximum 2θ value of 60.7° for **3**-$ClO_4\cdot C_2H_5CN$. A total of 720 oscillation images were collected. The first sweep of data was done using ω scans from −80.0 to 100.0° in 0.50° step, at $\chi = 45.0°$ and $\phi = 0.0°$. The second sweep of data was made using ω scans from −80.0 to 100.0° in 0.50° step, at $\chi = 45.0°$ and $\phi = 90.0°$. Crystal-to-detector distances were 35 mm, and detector swing angles were 10°. Exposure rates were 24.0, 26.0, and 40.0 s/deg for **1**-$CF_3SO_3\cdot CH_3CN$, **2**-BPh_4, and **3**-$ClO_4\cdot C_2H_5CN$, respectively. The data were corrected for Lorentz and polarization effects. Empirical absorption corrections were applied.

The structures were solved by a direct method (SIR92)[32] and expanded using a Fourier technique.[33] The structures were refined by a full-matrix least-squares method by using the teXsan[34] crystallographic software package (Molecular Structure Corporation). Non-hydrogen atoms of complex cations and counteranions were refined with anisotropic displacement parameters. Some non-hydrogen atoms of solvent molecules were refined with isotropic displacement parameters. Hydrogen atoms were positioned at calculated positions (0.95 Å). They were included, but not refined, in the final least-squares cycles. Crystallographic data are summarized in Table 1. ORTEP views (50% probability) of the complex cations of **1**-$CF_3SO_3\cdot CH_3CN$, **2**-BPh_4, and **3**-$ClO_4\cdot C_2H_5CN$ with full numbering scheme of atoms are shown in Figure S2, S3, and S4, respectively. Tables of final atomic coordinates, thermal parameters, and full bond distances and angles are given in the CIF Supporting Information file.

$[Cu_2(L3)_2(OH)_2](CF_3SO_3)_2\cdot CH_3CN$ (1-$CF_3SO_3\cdot CH_3CN$). A single crystal with approximate dimensions of 0.35 × 0.25 × 0.10 mm^3 was mounted on the tip of a glass rod. The asymmetric unit consists of a half of a $[Cu_2(OH)_2(L3)_2]^{2+}$ cation, a trifluoromethanesulfonate anion, and an acetonitrile molecule with half occupancy. Hydrogen atoms of acetonitrile were not included in the refinement. The maximum peak on a final difference Fourier map (1.14 e Å^{-3}) was observed near the acetonitrile molecule.

$[Cu_2(L3)_2(OOH)(OH)](BPh_4)_2\cdot 5(CH_3)_2CO\cdot 3H_2O$ (2-BPh_4). A single crystal with dimensions of 0.25 × 0.18 × 0.05 mm^3 was picked up from a solution by a nylon loop (Hampton Research Co.) on a handmade cold copper plate mounted inside a liquid N_2 Dewar vessel at ca. −80 °C and dipped quickly in liquid nitrogen. Then the crystal was mounted on a goniometer head in a N_2 cryostream. Although the complex cation has no center of symmetry, analysis revealed the presence of a center of symmetry due to disorder between the μ-1,1-OOH and μ-OH groups. The structure was solved by a model in which the bridging OOH ligands are equally disordered to give a chemically reasonable structure; the occupancies of O(1) and O(2) were estimated to be 1.0 and 0.5, respectively. There are one fully occupied and three half-occupied acetone molecules, and three half-occupied water molecules. The half-occupied acetone and water molecules were refined isotropically. The coordinates of the water molecules were fixed at the final least-squares

(32) *SIR-92*: Altomare, A.; Cascarano, G.; Giacovazzo, C.; Guagliardi, A.; Burla, M. C.; Polidori, G.; Camalli, M. *J. Appl. Crystallogr.* **1994**, *27*, 435.
(33) Beurskens, P. T.; Admiraal, G.; Beurskens, G.; Bosman, W. P.; de Gelder, R.; Israel, R.; Smits, J. M. M. *The DIRDIF-94 Program System*; Technical Report of the Crystallography Laboratory; University of Nijmegen: Nijmegen, The Netherlands, 1994.
(34) *teXsan: Crystal Structure Analysis Package*; Molecular Structure Corporation: The Woodlands, TX, 1985 and 1992.

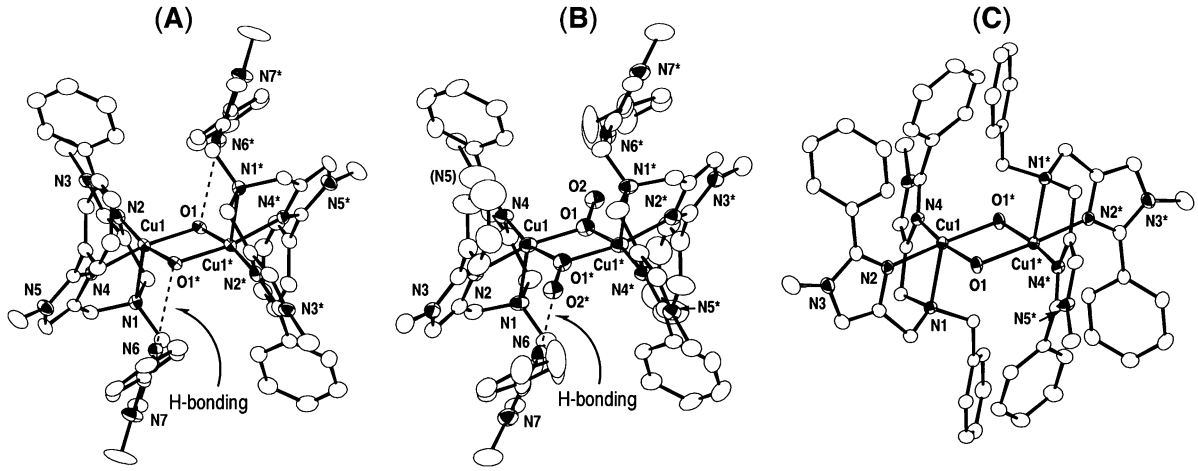

Figure 1. ORTEP views (50% probability) of the complex cations of (A) $[Cu_2(L3)_2(OH)_2](CF_3SO_3)_2\cdot CH_3CN$ (**1**-$CF_3SO_3\cdot CH_3CN$), (B) $[Cu_2(L3)_2(OOH)(OH)](BPh_4)_2\cdot 5(CH_3)_2CO\cdot 3H_2O$ (**2**-BPh_4), and (C) $[Cu_2(L1)_2(OH)_2](ClO_4)_2\cdot 2C_2H_5CN$ (**3**-$ClO_4\cdot C_2H_5CN$). Hydrogen atoms are omitted for clarity.

cycles. Hydrogen atoms of solvent molecules were not included in the refinement. The equivalent temperature factors (Ueq's) of some remote carbon atoms are large due to the disorder problem, whereas the ratio Ueq(max)/Ueq(min) of nonsolvent carbons was in the allowable range (3.4). The maximum peak on a final difference Fourier map (1.19 e $Å^{-3}$) was observed near a water molecule.

$[Cu_2(L1)_2(OH)_2](ClO_4)_2\cdot 2C_2H_5CN$ (3-$ClO_4\cdot C_2H_5CN$). A single crystal with approximate dimensions of $0.25 \times 0.20 \times 0.10$ mm^3 was picked up from the reaction solution and mounted on top of a glass fiber. An asymmetric unit consists of a half of a complex cation, a perchlorate anion, and a propionitrile molecule. The maximum peak on a final difference Fourier map (1.39 e $Å^{-3}$) was observed near a perchlorate anion. Although completeness of the data for $2\theta_{max} \leq 60.7°$ is lower (0.82), that for $2\theta_{max} \leq 55.93°$ is 0.96 and the high refln/param ratio (16.5) is enough for the sufficient structure quality.

Results and Discussion

Synthesis of Hydroperoxo−Dicopper(II) Complexes $[Cu_2(L3)_2(OOH)(OH)]^{2+}$ (2) and $[Cu_2(L1)_2(OOH)(OH)]^{2+}$ (4). Reaction of a bis(μ-hydroxo)dicopper(II) complex ($[Cu_2(L3)_2(OH)_2]^{2+}$ (**1**)) with H_2O_2 in acetonitrile at −40 °C generated a green complex $[Cu_2(L3)_2(OOH)(OH)]^{2+}$ (**2**). The electronic spectral measurement indicated that more than 5 equiv of H_2O_2 is needed for the complete formation of **2**. ESI-TOF/MS spectrum definitively confirmed the formation of **2** (m/z = 615.2, I = 100% for $\{Cu_2(L3)_2(OOH)(OH)\}^{2+}$ and m/z = 617.2 for $\{Cu_2(L3)_2(^{18}O^{18}OH)(OH)\}^{2+}$) (see Figure S5). It was also attempted to synthesize a bis(μ-1,1-hydroperoxo)dicopper(II) species or a mononuclear hydroperoxo−copper(II) species by treatment of a large excess of H_2O_2, whereas no such species was detected by ESI-TOF/MS. Thus, the present sterically hindered tetradentate tripodal ligand L3 selectively generates a (μ-1,1-hydroperoxo)(μ-hydroxo)dicopper(II) complex.

We have also tried to synthesize a (μ-1,1-hydroperoxo)(μ-hydroxo)dicopper(II) complex having a closely related tridentate ligand (L1) consisting of two 2-phenylimidazolyl groups (Scheme 1). Reaction of an acetonitrile solution of a bis(μ-hydroxo)dicopper(II) complex, $[Cu_2(L1)_2(OH)_2]^{2+}$ (**3**) (typically ~0.1 mM), with 10 equiv of 30% H_2O_2 at −40 °C generated a dark blue species. The electronic and Raman measurements suggested the formation of a hydroperoxo−copper(II) complex (vide infra). In addition, ESI-TOF/MS measurement showed a signal at m/z = 535.2 (I = 22%) for $\{Cu_2(L1)_2(OOH)(OH)\}^{2+}$ (**4**) and m/z = 537.2 for $\{Cu_2(L1)_2(^{18}O^{18}OH)(OH)\}^{2+}$.

Table 2. Selected Bond Distances and Angles of $[Cu_2(L3)_2(OH)_2](CF_3SO_3)_2\cdot CH_3CN$ (**1**-$CF_3SO_3\cdot CH_3CN$), $[Cu_2(L3)_2(OOH)(OH)](BPh_4)_2\cdot 5(CH_3)_2CO\cdot 3H_2O$ (**2**-BPh_4), and $[Cu_2(L1)_2(OH)_2](ClO_4)_2\cdot 2C_2H_5CN$ (**3**-$ClO_4\cdot C_2H_5CN$)

	1-$CF_3SO_3\cdot CH_3CN$	**2**-BPh_4	**3**-$ClO_4\cdot C_2H_5CN$
	Bond Distances (Å)		
Cu1−N1	2.450(4)	2.461(5)	2.411(2)
Cu1−N2	1.999(4)	1.996(5)	2.012(2)
Cu1−N4	2.017(4)	1.997(5))	1.972(2)
Cu1−O1	1.934(3)	1.942(4)	1.913(2)
Cu1−O1*	1.916(3)	1.919(4)	1.930(2)
Cu1···Cu2	2.927(1)	3.072(2)	3.013(2)
O1···O2		1.430(9)	
	Bond Angles (deg)		
Cu1−O1−Cu1*	98.9(1)	105.4(2)	103.24(8)
O1−Cu1−O1*	81.1(1)	74.6(2)	76.76(8)
O1−Cu1−N1	97.7(1)	99.4(2)	101.25(7)
Cu1−O1−O2		122.3(4)	
Cu1*−O1−O2		131.0(4)	

Structural Characterization of Complexes 1, 2, and 3. Figure 1 shows the structures of the complex cations of **1**-$CF_3SO_3\cdot CH_3CN$ (A), **2**-BPh_4 (B), and **3**-$ClO_4\cdot C_2H_5CN$ (C), and their selected bond distances and angles are given in Table 2. Complex cations of **1**-$CF_3SO_3\cdot CH_3CN$ and **3**-$ClO_4\cdot C_2H_5CN$ have a bis(μ-hydroxo)dicopper(II) core, and that of **2**-BPh_4 has a (μ-hydroxo)(μ-1,1-hydroperoxo)dicopper(II) core. Unfortunately, the bridging OOH and OH groups in **2**-BPh_4 are disordered with each other with 0.5 occupancy for the terminal oxygen of OOH. Although there is a possibility that the crystals consist of a mixture of **1** and bis(μ-1,1-hydroperoxo)dicopper(II) species $[Cu_2(L3)_2(OOH)_2]^{2+}$, ESI-TOF/MS measurement definitively confirmed the formation of **2** (see ESI-TOF/MS spectra in Figure S5). Each copper in these three complexes has a square pyramidal structure having an N_3O_2 donor set with a weak ligation of a tertiary amine nitrogen in the apex. Consequently, one pendant arm of L3 in **1**-$CF_3SO_3\cdot CH_3CN$ and **2**-BPh_4 is free from coordination, which produces a hydrophobic cavity around dicopper(II) core (vide infra). The $Cu_2(\mu\text{-}OH)_2$ and $Cu_2(\mu$-1,1-OOH)(μ-OH) core dimensions of these three complexes (Cu−O = 1.913−1.942 Å and Cu···Cu = 2.927−3.072 Å) are quite similar to each other and typical of those of the bis(μ-hydroxo)-dicopper(II) complexes.

Although detailed discussion about metric parameters of **2**-BPh_4 may not be warranted due to the disordered problem,

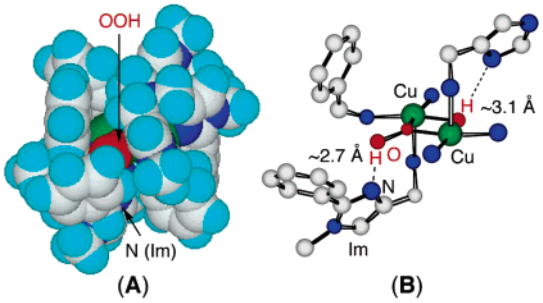

Figure 2. Space filling model (A) of **2** and ball-and-stick view (B) showing the hydrogen bondings. Green: copper, red: oxygen, dark blue: nitrogen, gray: carbon, and light blue: hydrogen. Hydrogen atoms in the space filling model were placed at the calculated positions, and the C−H bond distances are set to 1.10 Å.

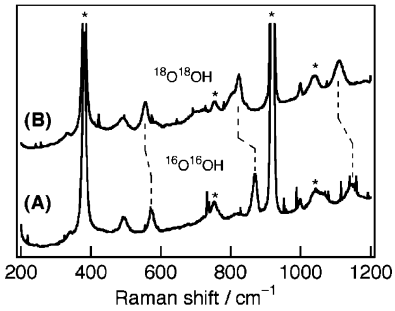

Figure 3. Resonance Raman spectra of **2** in acetonitrile at −40 °C prepared by $H_2{}^{16}O_2$ (A) and $H_2{}^{18}O_2$ (B) with a 406.7-nm laser excitation. The asterisk bands are solvent bands, and the spikes are noises.

the structural features are clear. The Cu(μ-1,1-OOH)(μ-OH) core is covered by a hydrophobic cavity formed by phenyl groups and pendant arms (Figure 2A), which is large enough to accommodate both μ-1,1-hydroperoxo and hydroxo groups without a significant stereochemical change. Such a large hydrophobic cavity may be responsible for the disordered structure. A striking structural feature in **2** is hydrogen bondings between the hydroperoxide and the imidazole nitrogen of the uncoordinated pendant arm in one side (N6···O2*(H) = ~2.7 Å) and between the hydroxide and the imidazole nitrogen of the uncoordinated pendant arm in the other side (N6*···O1(H) = ~3.1 Å) (Figures 1B and 2B). Similar hydrogen bondings between hydroxides and imidazole nitrogens are also present in **1** (N6···O1*(H) = ~2.9 Å). Unlike **1** and **2**, complex **3** containing the tridentate ligand (L1) has no hydrophobic cavity (see Figure S4), implying that hydrogen bonding is essential for the formation of the hydrophobic cavities of **1** and **2**.

Masuda and co-workers reported the first structurally characterized mononuclear hydroperoxo−copper(II) complex having a tetradentate tripodal ligand containing pivalamido groups ([Cu(bppa)(OOH)]$^+$),[10] in which hydrogen bonding between a coordinated oxygen (proximal oxygen) of hydroperoxide and two pivalamido NH hydrogens of the supporting ligand is also present. Although the hydrogen bonding mode of [Cu(bppa)-(OOH)]$^+$ in which the hydroperoxo ligand acts as a hydrogen bond acceptor differs from that of **2** in which the hydroperoxo ligand acts as a hydrogen bond donor, both hydrogen bondings can contribute the stabilization of the hydroperoxo complexes (vide infra). Recently, Masuda and co-workers also reported that the hydrogen bonding between the distal oxygen of hydroperoxo ligand and amide−hydrogen of the supporting ligand in [Cu(La)(OOH)]$^+$ where hydroperoxide acts as hydrogen bonding acceptor destabilizes the hydroperoxo−Cu(II) complex.[18] Thus, hydrogen bonding plays various roles for stabilization, destabilization, or activation of hydroperoxo ligands depending on the hydrogen bonding modes.

Resonance Raman and UV−Vis Spectroscopies of 2 and 4. The resonance Raman spectrum of $[Cu_2(L3)_2(OOH)(OH)]^{2+}$ (**2**) showed isotope-sensitive bands at 572 cm^{-1} ($^{16-18}\Delta$ = 16 cm^{-1}), 868 cm^{-1} ($^{16-18}\Delta$ = 45 cm^{-1}), and 1144 cm^{-1} ($^{16-18}\Delta$ = 34 cm^{-1}) as shown in Figure 3, and the resonance Raman and electronic spectral data of some mono- and dinuclear hydroperoxo−copper(II) complexes are given in Table 3. The former two bands are assignable to the Cu−O(OH)−Cu stretching vibration (ν_{as}(Cu−O)) and the O−O stretching vibration (ν(O−O)), respectively, by analogy to the features of a closely related dinuclear complex $[Cu_2(UN-O)(OOH)]^{2+}$ (**7**).[26] Although for **7**, ν_s(Cu−O) vibration was observed at 322 cm^{-1}, no ν_s(Cu−O) vibration was detected for **2**. The band at 1144 cm^{-1} is tentatively assigned to the overtone of the ν_{as}(Cu−O) vibration. Raman spectra of $[Cu_2(L1)_2(OOH)(OH)]^{2+}$ (**4**) also showed similar features at 562 cm^{-1} ($^{16-18}\Delta$ = 23 cm^{-1}), 883 cm^{-1} ($^{16-18}\Delta$ = 50 cm^{-1}), and 1120 cm^{-1} ($^{16-18}\Delta$ = 40 cm^{-1}) as shown in Figure S6. By analogy to the features of **2**, they can be assigned as the Cu−O(OH)−Cu stretching vibration (ν_{as}(Cu−O)), the O−O stretching vibration (ν(O−O)), and the overtone of the ν_{as}(Cu−O) vibration, respectively. The ν(O−O) values of **4** (883 cm^{-1}) and **7** (892 cm^{-1}) are significantly higher than that of **2** (868 cm^{-1}). The high ν(O−O) frequency of **7** has been explained in terms of the direct effect of protonation to the bridging peroxide.[26] The lower energy of the ν(O−O) vibration of **2** relative to those of **4** and **7** may be in line with hydrogen bonding which would leave some electron density on the π* orbital of the peroxo moiety, resulting in the decrease of the O−O bond order. In contrast, the ν_{as}(Cu−O) frequency of **2** (572 cm^{-1}) is higher than those of **4** (562 cm^{-1}) and **7** (506 cm^{-1}), suggesting the stronger donation of the bridging OOH of **2** compared to those in **4** and **7**. This is also in line with the presence of hydrogen bonding. The ν(O−O) frequencies of most of the mononuclear copper(II) complexes[10−18] reported thus far are in the range 865−835 cm^{-1} except for 881 cm^{-1} observed for $[Cu(N_3S)(OOH)]^+$.[15] The ν(O−O) frequencies of the dimers are higher than most of the mononuclear complexes, reflecting the stronger electron donation of the μ-1,1-OOH groups to two copper(II) ions compared to those of the monodentate OOH groups.

The electronic spectrum of **2** in acetonitrile at −40 °C (Figure 4 and Table 3) showed an intense band at 356 nm (ϵ = 6300 M^{-1} cm^{-1}) and a weak band at 580 nm (ϵ = 240 M^{-1} cm^{-1}) with a shoulder at 664 nm (ϵ = ~190 M^{-1} cm^{-1}), which are assigned as π_σ*(OOH)-to-Cu(II) LMCT[26] and d−d transitions, respectively, by analogy to the features of $[Cu_2(UN-O)-(OOH)]^{2+}$ (**7**). Similar spectral features are also observed for **4** (Table 3 and Figure S7). However, the π_σ*-to-Cu(II) LMCT transition energies of **2** and **4** are significantly higher than those of dinuclear copper(II) complexes having a phenolate bridge such as **7** (λ_{mas} = 395 nm (ϵ = 7000 M^{-1} cm^{-1})).[22−27] Such a high transition energy of **2** and **4** could be partly attributable to a stronger donation of the bridging OOH compared to that in **7**. Higher π_σ*-to-Cu(II) LMCT transition energy of **4** relative to that of **2** is not in line with the aforementioned notion given in Raman spectroscopy that hydrogen bonding in **2** increases

Table 3. Spectroscopic Data for Mononuclear and Dinuclear Hydroperoxo−Copper(II) Complexes

complexes	UV−vis λ_{max}/nm (ϵ/M^{-1} cm^{-1})	ν(O–O) ($^{16-18}\Delta$), ν(Cu–O) ($^{16-18}\Delta$) $\tilde{\nu}$/cm^{-1}	ref
$[Cu_2(L3)_2(OOH)(OH)]^{2+}$ (**2**)	356 (6300), 580 (240), 664 (sh ∼190)	868 (45), 572 (16)[a]	this work
$[Cu_2(L1)_2(OOH)(OH)]^{2+}$ (**4**)	341 (∼7000), 581 (∼170), 770 (sh ∼80)	883 (50), 562 (23)[a]	this work
$[Cu_2(UN-O)(OOH)]^{2+}$ (**7**)	395 (7000), 645 (660)	892 (55), 506 (15),[a] 322 (10)[b]	26
$[Cu_2(L)(OOH)]^{3+}$	342 (12000), 444 (1200), 610 (800)		28
$[Cu(bppa)(OOH)]^{+}$	380 (890), 660 (150), 830 (250)	856 (46)	10
$[Cu(tpa)(OOH)]^{+}$	379 (1700), 668 (170), 828 (200)	847 (55)	17
$[Cu(bpba)(OOH)]^{+}$	350 (3400), 564 (150), 790 (sh 55)	834	17
$[Cu(N_3S)(OOH)]^{+}$	357 (4300), 600 (140)	881 (49)	15
$[Cu(HB(3\text{-}tBu\text{-}5\text{-}^{i}Prpz)_3)(OOH)]^{+}$	600 (1540), 830 (∼300)	843 (44), 624 (17)	11

[a] ν_{as}(Cu−O) vibration. [b] ν_{s}(Cu−O) vibration.

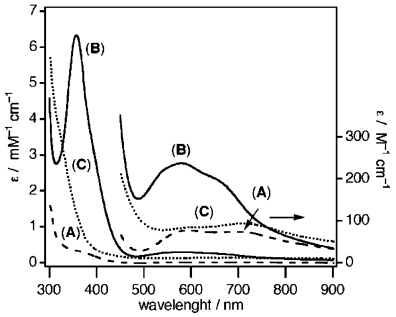

Figure 4. Electronic spectra of (A) **1** and (B) **2** in acetonitrile at −40 °C and (C) that of a decomposed product of **2** in acetonitrile at room temperature.

the electron donation of hydroperoxide, suggesting that some other factor(s) such as stereochemistry around copper(II) ions seems to be also important. Such a high LMCT transition energy has been suggested for a dinuclear copper(II) complex $[Cu_2(L)(OOH)]^{3+}$ (λ_{max} = 342 nm, ϵ = 12000 M^{-1} cm^{-1}), which can hydroxylate a xylyl linker.[28] A similar absorption band has also been found in the catalytic cycle of laccase (λ_{mas} = 340 nm (ϵ = 4500 M^{-1} cm^{-1})), in which a dinuclear Cu(II)(μ-1,1-OOH)Cu(I) species has been proposed as one of possible intermediates.[8] Thus, the LMCT transitions of dinuclear copper(II) complexes occur in a wide rang depending on stereochemistry around the copper(II) ion and the nature of hydroperoxide.

The LMCT of mononuclear hydroperoxo−Cu(II) complexes are observed in the range 380−350 nm except for that observed for a tetrahedral $[Cu(HB(3\text{-}tBu\text{-}5\text{-}^{i}Prpz)_3)(OOH)]^{+}$ (λ_{max} = 600 nm, ϵ = 1540 M^{-1} cm^{-1}).[11] Masuda and co-workers suggested that the LMCT transition energies depend on the stereochemistry of complexes; transition energies of the square planer and square pyramidal complexes such as $[Cu(bpba)(OOH)]^{+}$ [17] and $[Cu(N_3S)(OOH)]^{+}$ [15] are higher than those of trigonal bipyramidal complexes such as $[Cu(bppa)(OOH)]^{+}$ [10] and $[Cu(tpa)(OOH)]^{+}$.[17] The LMCT energies of **2** and **4** are comparable to those of mononuclear square planer and square pyramidal copper(II) complexes.

Effect of Hydrophobic Cavity on H/D and ^{16}O/^{18}O Exchange Reactions of Complexes 1 and 2. It is noted that the hydrophobic cavity supported by hydrogen bondings significantly influences the H/D and ^{16}O/^{18}O exchange reactions of the bridging hydroxide and/or hydroperoxide in **2**. Figure 5A shows the ESI-TOF/MS spectrum of an acetonitrile solution containing both **1** ($\{\mathbf{1}\text{-}(^{16}OH)_2\}^{2+}$) ($m/z$ = 607.2) and **2** ($\{\mathbf{2}\text{-}(^{16}OH)(^{16}O^{16}OH)\}^{2+}$) ($m/z$ = 615.2) at −40 °C (hereafter O stands for ^{16}O except for ^{16}O/^{18}O). Addition of D_2O caused a rapid H/D exchange from $\{\mathbf{1}\text{-}(OH)_2\}^{2+}$ (m/z = 607.2) to $\{\mathbf{1}\text{-}(OD)_2\}^{2+}$ (m/z = 608.2) within a few minutes (Figure 5B). Unlike **1**, surprisingly, only one H/D exchange occurred in **2** to generate $\{\mathbf{2}\text{-}(OD)(OOH)\}^{2+}$ or $\{\mathbf{2}\text{-}(OH)(OOD)\}^{2+}$ (m/z = 615.7) as shown in Figure 5, parts B and B′, indicating that the hydrophobic cavity of **2** prevents a rapid H/D exchange of either hydroperoxide or hydroxide. For complex **1**, a rapid ^{16}O/^{18}O exchange from $\{\mathbf{1}\text{-}(OH)_2\}^{2+}$ (m/z = 607.2) to $\{\mathbf{1}\text{-}(^{18}OH)_2\}^{2+}$ (m/z = 609.2) was also observed within a few minutes by reaction of $H_2{}^{18}O$ as expected for the substitution-labile copper(II) complexes via either associative or dissociative mechanism, whereas no ^{16}O/^{18}O exchange was observed for $\{\mathbf{2}\text{-}(OH)(OOH)\}^{2+}$ (Figure 6, parts B and B′). Thus the hydrophobic cavity of **2** has a significant protection effect on the H/D and ^{16}O/^{18}O exchange reactions. We further followed the time courses of the spectral changes of **2** in the presence of D_2O (Figure 5B−D and B′−D′) and in the presence of $H_2{}^{18}O$ (Figure 6B−D and B′−D′). In both cases, the intensities of the signals of **2** decreased with time (the presence of water accelerated the decomposition of **2** (vide infra)). In the presence of D_2O, the

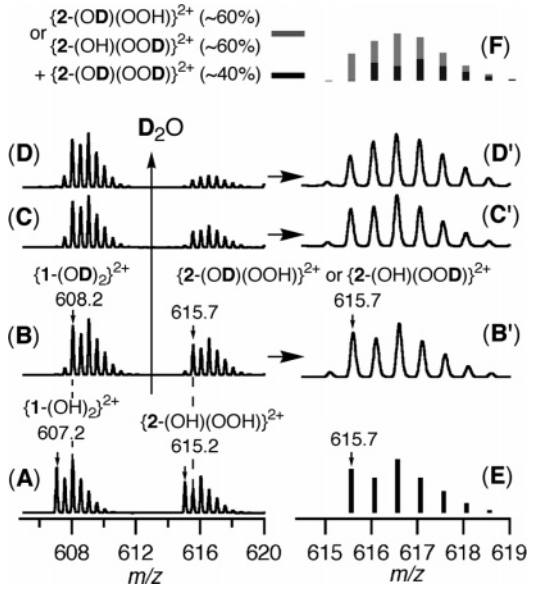

Figure 5. (A) ESI-TOF/MS spectrum of **1** and **2** in acetonitrile at −40 °C, (B−D) time course of the spectral changes in the presence of D_2O, (B′−D′) that in the $\{\mathbf{2}\text{-}(OH)(OOH)\}^{2+}$ region where the intensities of the signals (C′ and D′) are magnified for clarity, (E) theoretical isotope pattern of $\{\mathbf{2}\text{-}(OD)(OOH)\}^{2+}$ or $\{\mathbf{2}\text{-}(OH)(OOD)\}^{2+}$, and (F) a simulated spectrum of (C′) consisting of $\{\mathbf{2}\text{-}(OD)(OOH)\}^{2+}$ or $\{\mathbf{2}\text{-}(OH)(OOD)\}^{2+}$ (60%), and $\{\mathbf{2}\text{-}(OD)(OOD)\}^{2+}$ (40%). (B and B′): measured after ∼2 min after addition of D_2O, (C and C′): measured after 4 h, and (D and D′): measured after 12 h,. Sample preparation: (A) a solid sample of $\mathbf{2}\text{-}CF_3SO_3$ was dissolved into ∼1 mM acetonitrile solution of **1** (1 mL), and (B) an acetonitrile solution (∼600 μL) containing ∼20 μL of D_2O was mixed with the solution (A). The concentration of D_2O after the solutions are mixed is ∼630 mM.

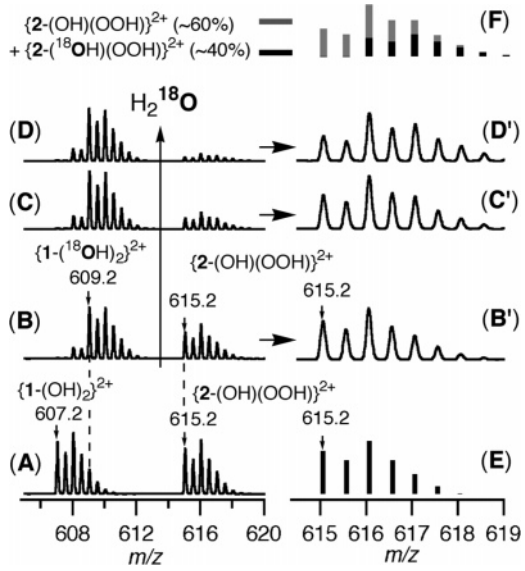

Figure 6. (A) ESI-TOF/MS spectrum of **1** and **2** in acetonitrile at −40 °C, (B−D) its time course of the spectral changes in the presence of $H_2{}^{18}O$, (B′−D′) that in $\{$**2**-(OH)(OOH)$\}^{2+}$ region where the intensities of the signals (C′ and D′) are magnified for clarity, (E) theoretical isotope pattern of $\{$**2**-(OH)(OOH)$\}^{2+}$, and (F) a simulated spectrum of (C′) consisting of $\{$**2**-(OH)(OOH)$\}^{2+}$ (60%) and $\{$**2**-(^{18}OH)(OOH)$\}^{2+}$ (40%). (B and B′): measured after ∼2 min after addition of $H_2{}^{18}O$, (C and C′): measured after 4 h, (D and D′): measured after 11 h. Sample preparation: (A) a solid sample of **2**-CF_3SO_3 was dissolved into ∼1 mM acetonitrile solution of **1** (1 mL), and (B) an acetonitrile solution (∼600 μL) containing ∼20 μL of $H_2{}^{18}O$ was mixed with the solution (A). The concentration of $H_2{}^{18}O$ after the solutions are mixed is ∼630 mM.

isotope patterns of **2** gradually change with time as shown in Figure 5, parts C′ and D′, measured after 4 and 12 h, respectively (cf. the theoretical stick spectrum E). The spectral change suggests the formation of **2**-(OD)(OOD); simulation of the isotope pattern given in Figure 5F shows that ca. 40% of conversion to **2**-(OD)(OOD) occurs after 12 h.[35] Thus the exchange rates of two hydrogens of hydroperoxide and hydroxide significantly differ due to the hydrophobic cavity supported by the hydrogen bondings. A similar isotope pattern change in the $^{16}O/^{18}O$ exchange reaction of **2** is also seen in Figure 6, parts C′ and D′, measured after 4 and 11 h, respectively (cf. theoretical stick spectrum E). Simulation of the isotope pattern (Figure 6F) also revealed that ca. 40% of the $^{16}O/^{18}O$ exchange of hydroxide occurs to generate **2**-(^{18}OH)(OOH). The results indicate that the exchange rate of the hydrogen of either hydroperoxide or hydroxide and that of the oxygen of hydroxide are slower than the decomposition rate of **2** and/or the exchange of these groups may be partly associated with decomposition of **2**. Thus the results clearly demonstrate that the hydrophobic cavity of **2** is robust and capable of suppressing the H/D and $^{16}O/^{18}O$ exchange reactions. Such a surprisingly robust hydrophobic cavity of **2** seems to be attributable to the stronger hydrogen bonding effect between the hydroperoxide and the uncoordinated imidazole nitrogen judging from the structural comparison of **1** and **2**. However, it is not clear at present why and how the combination of two types of the hydrogen bondings between the hydroperoxide and the imidazole nitrogen in one side and between the hydroxide and the imidazole nitrogen in the other side stabilizes the hydrophobic cavity of **2** compared to that of **1**, and why and how this hydrophobic cavity suppresses the H/D and $^{16}O/^{18}O$ exchange reactions. Nevertheless, the present results provide fundamental insights into the control of the ligand exchange reactions of the substitution-labile complexes by a hydrophobic cavity and the hydrogen bonding effect on the stability of the hydrophobic cavity. In addition, this hydrophobic cavity is also responsible for the enhanced thermal stability of **2** against decomposition compared to that of $[Cu_2(L1)_2(OOH)(OH)]^{2+}$ (**4**) having no hydrophobic cavity (vide infra).

(35) Prolonged standing for an additional 4 h revealed that further exchange reaction was still going on. Simulation of the isotope pattern of the spectrum measured after 16 h revealed that ca. 50% of conversion to **2**-(OD)(OOD) occurs (not shown in Figure 5).

Scheme 2 [a]

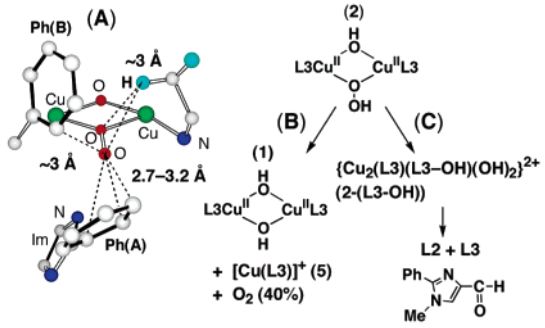

[a] (A) A ball-and-stick view of **2** showing the C···O_{OOH} and H···O_{OOH} distances close to the hydroperoxo group, where hydrogen atoms were placed at the calculated positions and the C−H bond distances are set to 1.10 Å. (B) and (C) Decomposition products of **2** in acetonitrile at 0 °C and in solid state at 60 °C.

Effect of Hydrophobic Cavity on Thermal Stability of 2 against Decomposition. Unlike **2**, $[Cu_2(L1)_2(OOH)(OH)]^{2+}$ (**4**) has no hydrophobic cavity around the $Cu_2(\mu$-1,1-OOH)(μ-OH) core. It is of interest to compare the relative thermal stabilities of **2** and **4** against decomposition. We measured the decomposition rates of **2** and **4** in the presence of water at 0 °C, since an acetonitrile solution of **4** generated by the reaction of 10 equiv of 30% H_2O_2 contains water. Both decomposition reactions of **2** and **4** follow first-order kinetics. Decomposition rate constants of **2** and **4** in acetonitrile at 0 °C in the presence of 120 equiv of H_2O are 8.0×10^{-4} s^{-1} and $\sim 8.2 \times 10^{-2}$ s^{-1}, respectively (see Figure S8). Thus, decomposition of **4** is ∼100 times faster than that of **2**. The results clearly indicate that the hydrophobic cavity supported by hydrogen bonding in **2** significantly stabilizes the $Cu_2(\mu$-1,1-OOH)(μ-OH) core against decomposition. Such a hydrophobic cavity has also been shown to be effective for stabilization of the unstable (μ-peroxo)diiron complexes[36] and high-valent bis(μ-oxo)dimetal complexes.[37]

Reactivity of 2-CF_3SO_3 in Acetonitrile and in Solid State. (a) Decomposition of 2-CF_3SO_3 in Acetonitrile. Since some $Cu(II)_2$−OOH species have been suggested to be reactive for aromatic hydroxylation, the reactivity of **2** toward the phenyl groups that are located in close proximity of the bridging OOH ($O_{terminal}$···C_{phenyl} = ∼2.7−3.2 Å) as shown in Scheme 2A is of particular interest. Decomposition of **2** in acetonitrile at 0 °C, however, resulted in no hydroxylation of the phenyl group,

(36) (a) Hayashi, Y.; Kayatani, T.; Sugimoto, H.; Suzuki, M.; Inomata, K.; Uehara, A.; Mizutani, Y.; Kitagawa, T.; Maeda, Y. *J. Am. Chem. Soc.* **1995**, *117*, 11220−11229. (b) Ookubo, T.; Sugimoto, H.; Nagayama, T.; Masuda, H.; Sato, T.; Tanaka, K.; Maeda, Y.; Okawa, H.; Hayashi, Y.; Uehara, A.; Suzuki, M. *J. Am. Chem. Soc.* **1996**, *118*, 701−702.

(37) (a) Shiren, K.; Ogo, S.; Fujinami, S.; Hayashi, H.; Suzuki, M.; Uehara, A.; Watanabe, Y.; Moro-oka, Y. *J. Am. Chem. Soc.* **2000**, *122*, 254−262. (b) Hayashi, H.; Fujinami, S.; Nagatomo, S.; Ogo, S.; Suzuki, M.; Uehara, A.; Watanabe, Y.; Kitagawa, T. *J. Am. Chem. Soc.* **2000**, *122*, 2124−2125.

but a ligand recovery experiment showed the formation of a small amount of an N-dealkylated ligand, bis(1-methyl-2-phenyl-4-imidazolylmethyl)amine (L2), which is generated via hydroxylation of a methylene group of L3 (vide infra). It was also found that dioxygen evolution (ca. 40% based on hydroperoxide) and reduction of **2** to copper(I) species $[Cu(L3)]^+$ (**5**: ca. 20% based on total copper) were detected, suggesting that the decomposition involves disproportionation of the hydroperoxo ligand and reduction of **2** to **5** by the hydroperoxo ligand.[38] The formation of **5** was confirmed by ESI-TOF/MS measurement (m/z = 590.2). The reactivity of **5**, which was separately synthesized, with dioxygen under the above experimental conditions is poor, and no measurable oxidation to copper(II) complex(es) was detected within the above time scale (a few hours). Such low dioxygen reactivity of **5** has also been reported for a closely related copper(I) complex having 6-phenylpyridyl groups $[Cu(TPPA)]^+$.[39] Although decomposition of **2** involves various pathways as mentioned above, the decomposition reaction in acetonitrile at 0 °C obeys first-order kinetics with respect to **2**. Addition of water accelerated the decomposition rate as shown in Figure S9 ($k_{obs} = 6.2 \times 10^{-4}$ s^{-1} in acetonitrile, $k_{obs} = 8.0 \times 10^{-4}$ s^{-1} in the presence of 120 equiv of water, and $k_{obs} = 1.4 \times 10^{-3}$ s^{-1} in the presence of 670 equiv of water). Thus, the decomposition reaction of **2** involves various pathways such as disproportionation of peroxide, reduction of **2** to copper(I), and so forth.

In contrast, decomposition of **2** in the presence of excess H_2O_2 had quite different results; decomposition of **2** in the presence of 20 equiv of H_2O_2 in acetonitrile at room temperature gave a brown solution. The ESI-TOF/MS spectrum of the brown solution showed a main signal at m/z = 605.2 (I = 100%) assignable to $\{Cu(L3 + O-H)\}^+$ together with a minor species having L3 ligand $\{Cu(L3)(CH_3CN)\}^{2+}$ (m/z = 605.2) as shown in Figure S10. An isotope labeling experiment using $H_2{}^{18}O_2$ revealed that the oxygen of $\{Cu(L3 + O-H)\}^+$ comes from $H_2{}^{18}O_2$. The electronic spectrum of the decomposed solution showed a shoulder at ~460 nm ($\epsilon \approx 350$ M^{-1} cm^{-1}) and ~670 nm ($\epsilon \approx 220$ M^{-1} cm^{-1}) as shown in Figure S11, where ϵ values are given as a monomer. The spectral feature is reminiscent of those of various mononuclear phenolato−copper(II) complexes (λ_{max} = 450−530 nm (ϵ = 2000−500 M^{-1} cm^{-1})).[40] The combination of ESI-TOF/MS and UV−vis results suggests the partial hydroxylation of a phenyl group in L3. The results indicate the formation of some other reactive species capable of the arene hydroxylation. Further studies are in progress.

(b) Decomposition of 2-CF_3SO_3 in Solid State and Identification of a Decomposed Complex 2-(L3-OH). Various unfavorable decomposition reactions occurred simultaneously in acetonitrile as mentioned above. However, it is expected that solvent-dependent unfavorable decompositions could be suppressed in the solid state thermolysis. Warming a solid sample of **2**-CF_3SO_3 at 60 °C for 1 h gave a complex having a

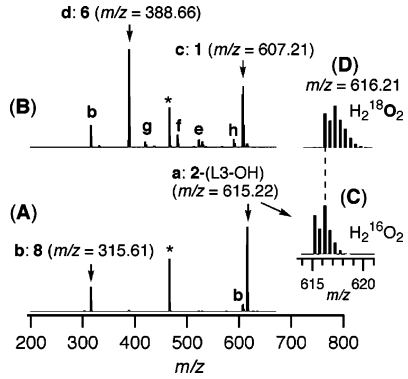

Figure 7. ESI-TOF/MS spectra of **2**-(L3-OH) in acetonitrile (A) at −40 °C and (B) at 20 °C. (C and D) ESI-TOF/MS spectra of **2**-(L3-OH) obtained from **2**-(OOH) and **2**-($^{18}O^{18}OH$), respectively. (a) **2**-(L3-OH) $\{Cu_2(L3)(L3\text{-}OH)(OH)_2\}^{2+}$ (m/z = 615.22), (b) **8** $\{Cu(L3)(CH_3CN)\}^{2+}$ (m/z = 315.61), (c) **1** $\{Cu_2(L3)_2(OH)_2\}^{2+}$ (m/z = 607.21), (d) **6** $\{Cu(L2)_2\}^{2+}$ (m/z = 388.66), (e) $\{Cu_2(L3)(L2)(OH)_2\}^{2+}$ (m/z = 522.17), (f) $\{Cu_2(L2)_2(Phim\text{-}CHO)\}^{2+}$ (m/z = 481.70), (g) $\{Cu(L2)\}^+$ (m/z = 420.12), (h) $\{Cu(L3)\}^+$ (m/z = 590.21). The asterisk (*) is an internal standard signal $\{(CH_3\text{-}(CH_2)_7)_4N\}^+$ (m/z 466.5352).

hydroxylated ligand $[Cu_2(L3)(L3\text{-}OH)(OH)_2]^{2+}$ (**2**-(L3-OH)) as a main product, where L3-OH is an oxidized ligand in which one of the methylene groups of the pendant arms is hydroxylated (Scheme 2C). Identification of **2**-(L3-OH) was carried out as follows. The ESI-TOF/MS spectrum of an acetonitrile solution of **2**-(L3-OH) at −40 °C showed a prominent peak at m/z = 615.22 ($\{Cu_2(L3)(L3\text{-}OH)(OH)_2\}^{2+}$, I = 100%) together with $\{Cu(L3)(CH_3CN)\}^{2+}$ (**8**, m/z = 315.61) as shown in Figure 7A, the former of which is the same mass number as that of **2**. However, the ESI-TOF/MS spectrum of **2**-(L3-OH) obtained from **2**-($^{18}O^{18}OH$) showed the presence of only one ^{18}O and no scrambling with ^{16}O (Figure 7D: m/z = 616.21), indicating that **2**-(L3-OH) has no $^{18}O^{18}OH$ group and a hydroxide generated after hydroxylation of the methylene group can be readily exchanged by adventurous water present in an acetonitrile solution. The H/D and $^{16}O/^{18}O$ exchange reactions of **2**-(L3-OH) in acetonitrile at −40 °C showed that **2**-(L3-OH) has three H/D exchangeable hydrogens and only one $^{16}O/^{18}O$ exchangeable oxygen (see Figure S12), suggesting that for **2**-(L3-OH), a hydrophobic cavity remains intact and influences the $^{16}O/^{18}O$ exchange reaction. Complex **2**-(L3-OH) is only stable at low temperature in acetonitrile. Warming the acetonitrile solution of **2**-(L3-OH) at room temperature caused a drastic spectral change as shown in Figure 7B. The main m/z = 615.22 signal corresponding to **2**-(L3-OH) ($\{Cu_2(L3)(L3\text{-}OH)(OH)_2\}^{2+}$) disappeared, and a new signal appeared at m/z = 388.7 as a main signal, which corresponds to a monomeric copper(II) species containing two N-dealkylated ligands, bis(1-methyl-2-phenyl-4-imidazolylmethyl)amine (L2), $[Cu(L2)_2]^{2+}$ (**6**) together with other minor species. Formation of $[Cu(L2)_2]^{2+}$ (**6**) was confirmed by comparison with **6** prepared separately. Ligand recovery experiments confirmed the formation of the N-dealkylated ligand (L2: yield = ~80% based on **2**) and 1-methyl-2-phenyl-4-formylimidazole (Phim-CHO). Isotope labeling experiment by **2**-($^{18}O^{18}OH$) showed that the oxygen atom in Phim-CHO comes from $^{18}O^{18}OH$, as mentioned in the Experimental Section. These experimental results clearly indicate that the hydroxylation occurs at the methylene position, and **2**-(L3-OH) can be formulated as $[Cu_2(L3)(L3\text{-}OH)(OH)_2]^{2+}$. Thus the aliphatic hydroxylation by **2** is in contrast to the arene

(38) Such a facile reduction of **2** may be partly attributable to strong hydrogen bonding between the hydroperoxide and the imidazole nitrogen, which makes the hydroperoxide a stronger reductant. In addition, a proton released upon reduction neutralizes synchronously the bridging hydroxide, leading to the stabilization of the copper(I) complex **5**.

(39) Chuang, C.-L.; Lim, K.; Chen, Q.; Zubieta, J.; Canary. J. W. *Inorg. Chem.* **1995**, *34*, 2562−2568.

(40) See, for example: (a) Itoh, S.; Taki, M.; Fukuzumi, S. *Coord. Chem. Rev.* **2000**, *198*, 3−20. (b) Jazdzewski, B. A.; Tolman, W. B. *Coord. Chem. Rev.* **2000**, *200−202*, 633−685.

Scheme 3. Possible Reaction Intermediates

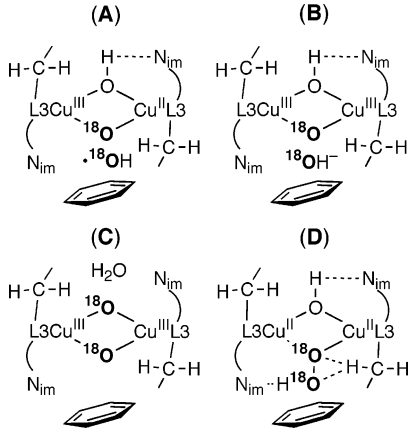

hydroxylation by some (μ-1,1-hydroperoxo)dicopper(II) complexes with a xylyl linker.

Mechanistic Considerations. For regioselective aliphatic hydroxylation performed by a solid sample of **2**, various reactive intermediates derived from the (μ-1,1-OOH)(μ-OH)Cu(II)$_2$ species may be considered, as shown in Scheme 3A−D. The homolytic O−O bond cleavage of the hydroperoxide would generate a hydroxy radical •OH (A), which is highly reactive and not selective for various substrates.[41] If this is the case, both the methylene and phenyl groups located in close proximity of the OOH (Scheme 2A) may be hydroxylated. Since no phenyl hydroxylation was observed in the solid state thermolysis and such a homolytic cleavage has been suggested to be energetically unfavorable,[8] this pathway seems unlikely. The heterolytic O−O bond cleavage is also possible, which could generate a high valent (μ-hydroxo)(μ-oxo)Cu(III)$_2$ species (B in Scheme 3). Although such a species has not yet been identified, the formation of this species may not be excluded in the solid state thermolysis. Another high valent bis(μ-oxo)Cu(III)$_2$ species (C) may also be generated by an alternative pathway; displacement of the hydroxide with the hydroperoxide could lead to the conversion to (μ-η^2:η^2-peroxo)Cu(II)$_2$ or trans-(μ-peroxo)Cu(II)$_2$ species, where the synchronous deprotonation from the hydroperoxide and the protonation to the hydroxide are needed. The O−O bond cleavage of the above peroxo complex could produce a bis(μ-oxo)Cu(III)$_2$ species. Such bis(μ-oxo)Cu(III)$_2$ species have been shown to be capable of aliphatic hydroxylation of supporting ligands.[9,42] A further possible pathway would be a direct reaction between an H atom of the methylene group and Cu(II)$_2$−OOH. The closest H atom of the methylene group is located within ~3 Å from both distal and proximal oxygens of the hydroperoxide (Schemes 2A and 3D). Thus, **2** has the potential possibility to generate the species having a variety of reactive oxygen species, which would be consistent with the observation that **2**-(^{18}O^{18}OH) gave only L3−^{18}OH ligand. Since aliphatic ligand hydroxylation by bis(μ-oxo)dicopper(III) species has been well-established, the present aliphatic ligand hydroxylation in **2** may proceed via intermediate (C) shown in Scheme 3. However, it is difficult to definitively identify the reactive intermediate from the current data.

It should be noted that some (μ-1,1-hydroperoxo)Cu(II)$_2$ species having xylyl linkers have been proposed to be reactive for hydroxylation of the xylyl linker as already mentioned. Casella and co-workers have proposed that the hydroxylation occurs through a direct overlap between the arene HOMO and the peroxide σ* component.[28] In contrast, no arene hydroxylation occurred for **2**, although **2** has a phenyl group Ph (A) (Scheme 2A) in close proximity of the hydroperoxide and their orientations seem to be suitable for a direct overlap of those two orbitals.

Summary

We have succeeded in preparation and isolation of a novel (μ-1,1-hydroperoxo)(μ-hydroxo)dicopper(II) complex **2** by the reaction of bis(μ-hydroxo)dicopper(II) complex **1** with H_2O_2 and its structural and spectroscopic characterization. Both Cu$_2$(μ-OH)$_2$ and Cu$_2$(μ-1,1-OOH)(μ-OH) cores in **1** and **2** are almost completely covered by the hydrophobic cavities formed by phenyl groups and uncoordinated pendant arms, which are preserved by hydrogen bondings. Unusually slow H/D and ^{16}O/^{18}O exchange reactions were observed for **2**, but not for **1**, indicating that the hydrophobic cavity of **2** is capable of suppressing the H/D and ^{16}O/^{18}O exchange reactions. Although the origin of such slow exchange reactions due to the hydrophobic cavity of **2** is not known at present, the results provide fundamental insights into the hydrophobic cavity effect on the ligand exchange reactions of the substitution-labile complexes and the hydrogen bonding effect on the robustness of the hydrophobic cavity. It was also found that the hydrophobic cavity of **2** significantly enhances the thermal stability against decomposition compared to **4**, which has no hydrophobic cavity.

The decomposition study of complex **2** provides new insights into the reactivity of hydroperoxide performed by the (μ-1,1-hydroperoxo)Cu(II)$_2$ complexes. Decomposition of **2** in acetonitrile resulted in the reduction of **2** to a copper(I) species and the disproportionation of hydroperoxide probably triggered by the displacement of the hydroperoxide with solvent or water molecule, and only a trace amount of ligand oxidation was observed. In contrast, decomposition of **2** in solid state at 60 °C showed the regioselective hydroxylation of the methylene group of the pendant arm in ~80% yield. This is the first example of the aliphatic hydroxylation of the supporting ligand by Cu$_2$−OOH species. This behavior is in marked contrast to those reported for some (μ-1,1-hydroperoxo)Cu(II)$_2$ complexes capable of the arene hydroxylation. It is noted that decomposition of **2** in the presence of excess of H_2O_2 in acetonitrile at room temperature caused a partial hydroxylation of the phenyl group of L3 ligand, indicating the formation of some other reactive species capable of the arene hydroxylation. For fuller understanding of the reactivity of the (μ-1,1-hydroperoxo)Cu(II)$_2$ species, it is necessary to investigate the details of such differential reactivities of the (μ-1,1-hydroperoxo)Cu(II)$_2$ species and the various reactive species derived from the (μ-1,1-hydroperoxo)Cu(II)$_2$ species.

(41) Ingold K. U.; MacFaul, P. A. In *Biomimetic Oxidations Catalyzed by Transition Metal Complexes*; Meunier, B., Ed.; Imperial College Press: London, 2000; pp 45−89.

(42) See, for example: (a) Tolman, W. B. *Acc. Chem. Res.* **1997**, *30*, 227−237. (b) Que, L., Jr.; Tolman, W. B. *Angew. Chem., Int. Ed.* **2002**, *41*, 1114−1137. (c) Itoh, S.; Fukuzumi, S. *Bull. Chem. Soc. Jpn.* **2002**, *75*, 2081−2095. (d) Lewis, E. A.; Tolman, W. B. *Chem. Rev.* **2004**, *104*, 1047−1076. (e) Mirica, L. M.; Ottenwaelder, X.; Stack, T. D. *Chem. Rev.* **2004**, *104*, 1013−1045. (f) Hatcher, L. Q.; Karlin, K. D. *J. Biol. Inorg. Chem.* **2004**, *9*, 669−683.

Acknowledgment. This work was partly supported by Grants-in-Aid for Scientific Research from the Ministry of Education, Science, and Culture, Japan (M.S., H.F., and T.K.).

Supporting Information Available: Twelve figures showing ORTEP and space-filling views of (**1**-$CF_3SO_3 \cdot CH_3CN$), (**2**-BPh_4), and (**3**-$ClO_4 \cdot C_2H_5CN$); ESI-TOF/MS spectrum of **2**; resonance Raman spectra of **4**; electronic spectra of **3** and **4**; electronic spectral change for the decomposition of **4** and **2**; ESI-TOF/MS spectra of the brown acetonitrile solutions obtained from decomposition of **2**; electronic spectra of **2** and a brown species obtained after warming at 20 °C; ESI-TOF/MS spectra of **2**-(L3-OH); and X-ray crystallographic files (PDF, CIF) This material is available free of charge via the Internet at http://pubs.acs.org.

JA047437H